Aust. J. Mar. Freshw. Res., 1986, **37**, 27–37

Pressure Fluctuations on the Open-ocean Floor: Mid-Tasman Sea at 38°30′S.,162°38′E., Near the Lord Howe Rise

F. E. M. Lilley,[A] *P. J. Mulhearn,*[B] *J. H. Filloux,*[C] *N. L. Bindoff*[A] *and I. J. Ferguson*[A]

[A] Research School of Earth Sciences, Australian National University, Canberra, A.C.T. 2601.
[B] Royal Australian Navy Research Laboratory, Pyrmont, N.S.W. 2010.
[C] Scripps Institution of Oceanography, University of California, San Diego, La Jolla, California 92093, U.S.A.

Abstract

A record, of 114 days duration, of pressure fluctuations on the floor of the Tasman Sea has been obtained from December 1983 to March 1984 at a site (38°30′S.,162°38′E.) near the Lord Howe Rise. The pressure fluctuations are due primarily to the ocean tides, and a first analysis of the record reveals clearly resolved open-ocean amplitude and phase values for four of the diurnal and semi-diurnal tidal components, namely Q_1, O_1, N_2 and M_2. Such observational results are important for comparison with global tidal models, and may allow their refinement, especially because tides in the seas around New Zealand are known to be complex. For the present site there is general agreement between the tidal results and the predictions of Schwiderski.

The pressure record also shows seismic signals from a strong earthquake that occurred on 7 February 1984 in the Solomon Islands, at a distance of approximately 3000 km from the pressure-record site. The detection of the seismic signals demonstrates the response and versatility of the pressure instrument used, and raises the possibility of its use in a different recording mode to study such seismic-generated pressure events more fully.

Introduction

This paper follows three earlier publications (Filloux 1980, 1983, 1984), which presented pressure fluctuations measured in the Pacific Ocean. The observation sites were on the open ocean floor near Hawaii, off the Gulf of California, and at the semi-diurnal amphidrome of the north-east Pacific. The instruments used were Bourdon tube-type transducers. For the measurements described in the present paper, a similar instrument (of least-count resolution 0·0390 cm seawater head equivalent) was operated in the Tasman Sea between Australia and New Zealand, just south of the southern flank of the Lord Howe Rise, at position 38°30′S., 162°38′E. in water of depth 4780 m. Concurrent with the measurement of pressure fluctuations reported here, other instruments positioned along a traverse from the Lord Howe Rise to eastern Australia recorded electric and magnetic fluctuations on the Tasman seafloor and on the Australian continent. The total experiment comprises a magnetotelluric study of electromagnetic induction in the oceans and in the solid earth, and is termed the Tasman Project of Seafloor Magnetotelluric Exploration (Graham 1984).

The site at which the data of the present paper were recorded is known as site TP2 in the context of the larger experiment, and is shown in Fig. 1. The instrument was deployed from the Australian naval oceanographic vessel HMAS *Cook* on 6 December 1983 (local date), and sank freely to the ocean floor to begin recording. Recovery was by the same vessel on 31 March 1984 (local date), when the instrument surfaced, having floated up from the ocean floor after detachment from its ballast tripod by preset timer command.

0067-1940/86/010027$02.00

In the present paper, the data of the 114-day recording period thus obtained (the recordings of the first day on the seafloor having been set aside as a period of stabilization) are presented and analysed. For more detailed discussion and description of the instrument characteristics, especially in relation to drift and temperature sensitivity, the reader is referred to Filloux (1980, 1983).

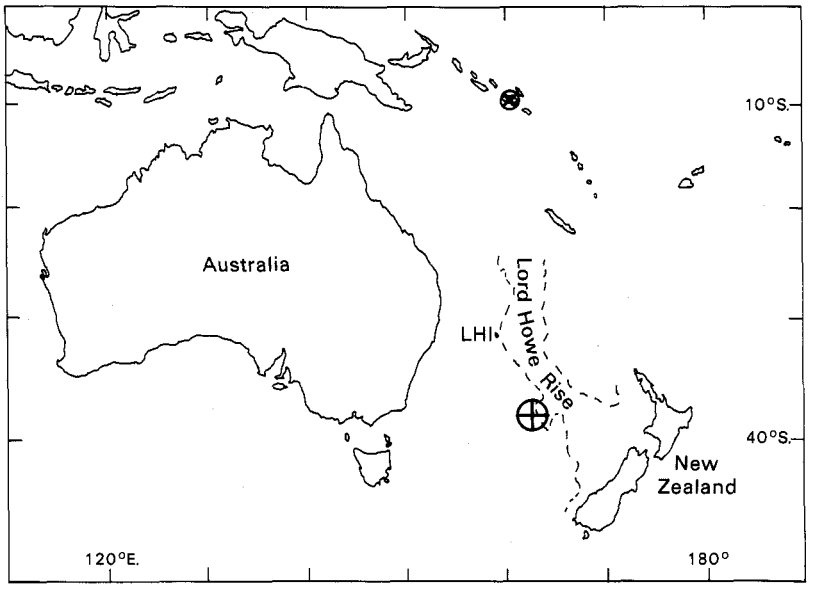

Fig. 1. Map showing the site (⊕) of the pressure-fluctuation measurements in the Tasman Sea. - - - 2000 m depth contour of the nearby Lord Howe Rise. LHI, Lord Howe Island. ⊗ Epicentre in the Solomon Islands of the earthquake of 7 February 1984.

The basic pressure readings were recorded in the instrument on magnetic tape at a rate of 128 readings per hour. The method of pressure measurement is such that each reading is a mean pressure value for the preceding $28\frac{1}{8}$ s of time. These data have been transcribed, decoded from their compact form of recording, and then edited for obvious accidental imperfections in the digital record (involving approximately 100 erroneous data points out of a total of order 350 000). The data then form the time series plotted in Fig. 2*a*.

Tidal signals dominate the record, and these will be analysed first below. Closer inspection of the data than is possible in Fig. 2 also shows other important signals, and these will be discussed in subsequent sections.

Tides

Two basic approaches can be taken to the analysis for tidal effects of data such as shown in Fig. 2*a*. One approach is to carry out a spectral analysis (such as by fitting Fourier series coefficients to the data), to indicate periodicities. The second approach, more refined in its determination of tidal component amplitude and phase, is to presume that tidal effects will be present at the known periods of the global tides. Then the best-fitting amplitudes and phases for these specified tidal components can be found by methods of least squares.

Both approaches have been followed in this paper, but it has first been necessary to estimate (and remove) a baseline drift for the data.

Baseline Drift

The data of Fig. 2*a* are shown plotted in compressed form in Fig. 2*b*, to make baseline drift more evident. Comparison of this figure with diagrams in the earlier papers (Filloux 1980 fig. 1, 1983 fig. 3) emphasizes how very much reduced is the drift in the present case, a result of continued transducer optimization.

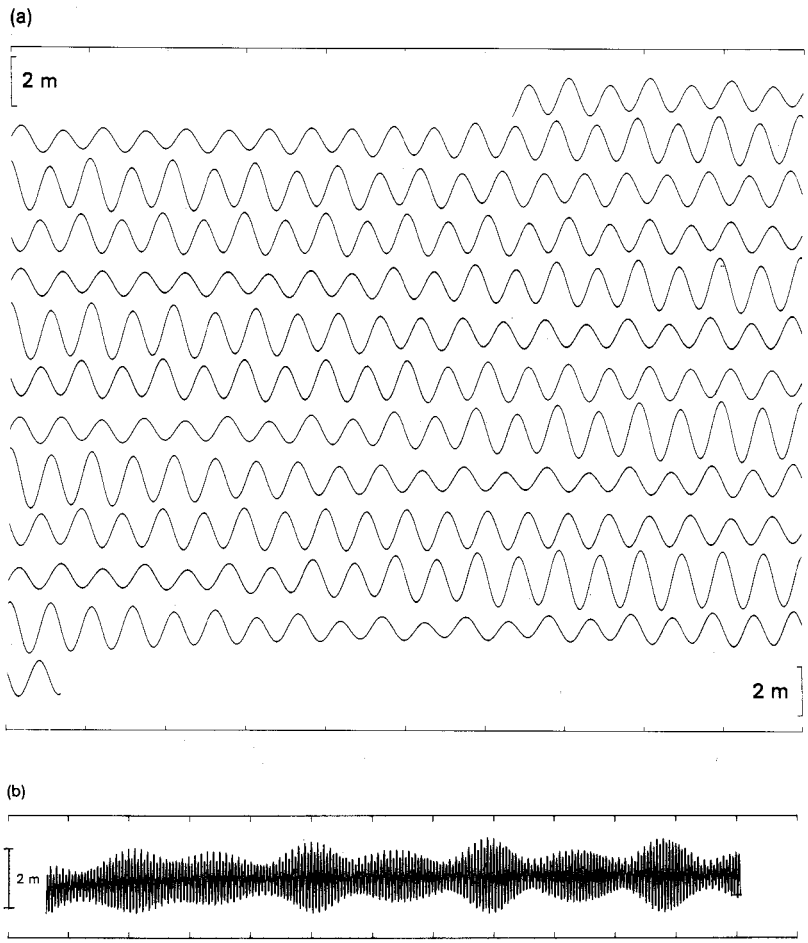

Fig. 2. (*a*) Plot of the pressure-fluctuation data. The span of each full horizontal trace is 10 days of record, and the traces are consecutive from top to bottom of the figure. The top trace starts at 07 h 30 min on 7 December 1983 UT, and the bottom trace ends at 16 h 30 min on 30 March 1984 UT. The two vertical scales, at the left-hand side of the top trace and the right-hand side of the bottom trace, are each for a pressure change of 2 m (seawater head quivalent). The horizontal scales are marked in days UT. (*b*) The pressure-fluctuation data plotted in compressed form. The horizontal scale marks are now at intervals of 10 days (starting at 0000 on 1 December 1983 UT). The vertical scale is for 2 m seawater head equivalent.

Many different approaches are possible to estimate and remove such drift. The results that follow are based on the procedure, considered supported by the drift displayed in Fig. 2*b*, of commencing analysis at 0000 Universal Time (UT) on 21 December 1983, and then subtracting

a linear drift defined as joining the mean of the first 5 days under analysis to the mean of the last 5 days under analysis.

Another computational technique in the present analysis of the data at tidal periods has been the use of quarter-hourly and half-hourly mean values, formed from the basic data by taking arithmetic means of the data recorded over every quarter-hour and every half-hour.

Fourier Coefficients

Subtracting a baseline drift as described above, and fitting standard Fourier coefficients to 4096 half-hourly mean values (starting with the first half-hour of 21 December 1983 UT) then produces the spectrum given in Fig. 3. Any periodicities thus found will necessarily be at harmonics of the original data length analysed, but within this limitation the method is thorough in its examination of the data.

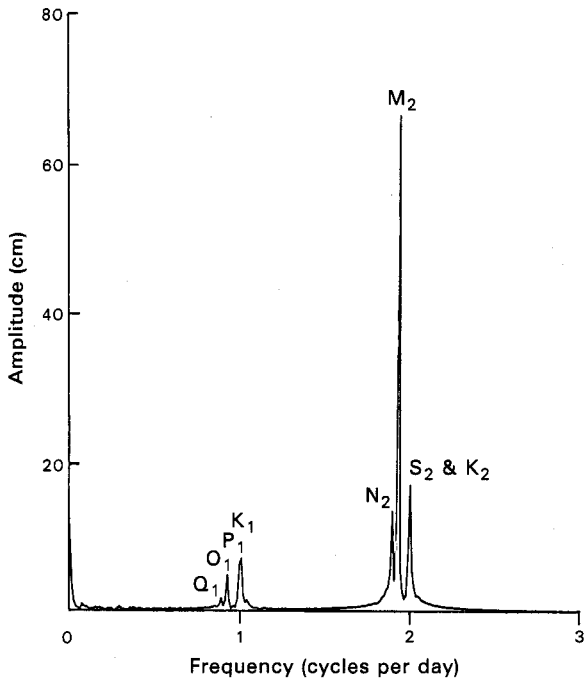

Fig. 3. Envelope of the amplitudes of Fourier coefficients fitted to the data on Fig. 2*b* as described in the text. The main peaks are marked with the tide notation for the periods at which they occur. More details are included in Table 1.

The amplitudes plotted at discrete intervals of frequency in Fig. 3 are the moduli of complex Fourier coefficients determined according to the definition

$$X_{k+1} = (2/N) \sum_{j=0}^{N-1} A_{j+1} \exp(2\pi ijk/N), \qquad k = 0, 1, \ldots, N-1,$$

where the input data A_{j+1} ($j = 0, 1, \ldots, N-1$) are the half-hourly mean values described, N has the value 4096 in the present case, and i denotes $(-1)^{1/2}$. The Fourier coefficient amplitude $|X_{k+1}|$ is then associated with a period of N/k input data intervals, that is a period of $N/2k$ hours.

The amplitude and phase values for the main tidal peaks evident in Fig. 3 are listed in Table 1. The phase values are given as lags relative to the appropriate tide at Greenwich (computed following Doodson and Warburg 1941, p. 40). The particular benefit of Fig. 3 is its direct demonstration that the main tidal components are all present, and that the data record is free from other periodic signals of comparable amplitude.

Analysis for Given Periods

Starting again with the first quarter-hour of 21 December 1983, and taking the time series of quarter-hourly mean values through to the end of the record, the data have then been used

Table 1. Amplitude and phase values for the eight main tidal components obtained from the pressure data for the mid-Tasman Sea site

The table compares the results from Fourier analysis with those from least-squares determination for given periods. Phases are lags in hours behind the appropriate equilibrium tide at Greenwich. Due to the proximity of the P_1 and K_1 tidal periods, and of the S_2 and K_2 tidal periods, the results for these components are provisional subject to further analysis. The results of the Fourier analysis in brackets correspond to peaks not clearly distinct in Fig. 3

Tidal component	Known period (h)	Details of nearest peak in Fig. 3 (Fourier analysis)			Least-squares result (given periods)	
		Period (h)	Amp. (cm)	Phase (h)	Amp. (cm)	Phase (h)
Q_1	26·8684	26·9474	1·8	19·5	1·3	21·6
O_1	25·8193	25·9241	4·8	15·9	5·1	20·6
P_1	24·0659	{ 24·0941	6·2	17·4 }	2·6	20·9
K_1	23·9345	{ 23·8140	6·9	3·9 }	9·9	23·1
N_2	12·6584	12·6420	13·1	12·2	14·4	11·4
M_2	12·4206	12·4121	63·8	11·1	65·6	10·9
S_2	12·0000	{ 12·0471	7·2	6·9 }	14·7	11·3
K_2	11·9672	{ 11·9766	16·4	7·2 }	6·5	11·8

to determine, by a least-squares procedure, amplitude and phase values for the main tidal components at exactly their known periods (taken from Godin 1972, p. 232). The results of this determination for the components identified in Fig. 3 are also listed in Table 1. As would be expected, there is general agreement between the Fourier coefficient and the least-squares results, with the latter being expected to be more accurate, especially for the tidal components close to each other in period, such as P_1 and K_1, and S_2 and K_2. No other observational results are known for open-ocean tides in the area, so that the results of Table 1 have a unique character.

Comparison with Tidal Models

In Table 2, the results for the four clearly resolved tidal components found by least squares are listed again, with results for a range of published global models of the ocean tides. These model results are given for the purposes and interest of comparison. However, the models vary in the methods by which they have been derived, and indeed in the accuracy which might be expected of them for the Tasman Sea. The Tasman Sea has been noted by many authors (e.g. Bye and Heath 1975) as an interesting and unusual tidal area, as the M_2 tidal phase circles around New Zealand. In the models of Accad and Pekeris (1978), the M_2 amplitude predicted on the eastern side of the Tasman Sea is the greatest for any part of the oceans not influenced by local coastal effects.

Generally in Table 2 there is reasonably good agreement (in some cases excellent agreement) between observed phase and model phase. There is also good agreement between observed amplitude and predicted amplitude for the diurnal tides. For the semi-diurnal tides, of which the dominant component M_2 has received most attention, the discrepancies between observed amplitude and model amplitude are substantial in some cases. Fig. 4 shows the present observation site plotted on the relevant part of the M_2 global tide map of Accad and Pekeris (1978), which has been calculated on the basis of tidal theory alone.

Table 2. Results for four mid-Tasman Sea tidal components compared with various published models
Amplitudes are given in centimetres, and phases are lags in hours behind the appropriate equilibrium tide at Greenwich

Tidal component		Present study	Values for tidal component: Bye and Heath (1975, figs 1 and 4)	Zahel (1977)	Accad and Pekeris (1978)	Parke and Hendershott (1980)	Schwiderski (1979, 1981*a*, 1981*b*, 1981*c*)
Q_1	Amp.	1·3					1·4
(26·8684 h)	Phase	21·6					20·7
O_1	Amp.	5·1					5
(25·8193 h)	Phase	20·6					21·3
N_2	Amp.	14·4					12
(12·6584 h)	Phase	11·4					10·6
M_2	Amp.	65·6	43	150	100	50	63
(12·4206 h)	Phase	10·9	9·0	10·4	9·8	10·4	10·9

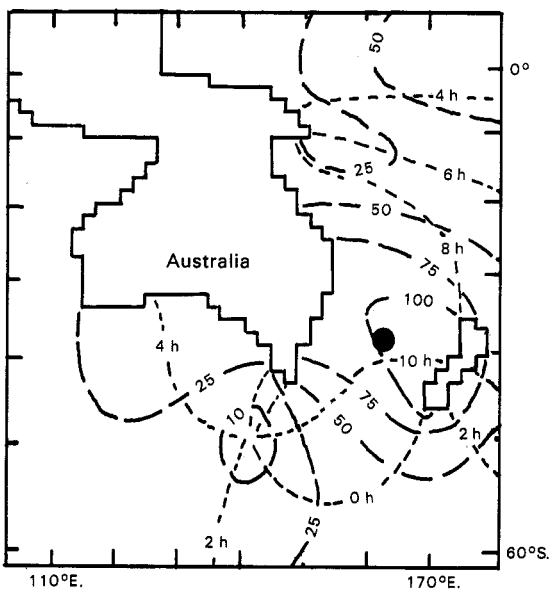

Fig. 4. Theoretical M_2 tide for the Tasman Sea, taken from the global results of Accad and Pekeris (1978, fig. 8). ——— Co-range lines, marked in units of cm (evidently used by Accad and Pekeris in the sense of being marked in units of amplitude). - - - - Co-tidal lines, marked in units of hours of phase lag behind M_2 (equilibrium) at Greenwich. ● Site of the present observations.

Accad and Pekeris (1978) discuss an observed M_2 tidal amplitude value for Lord Howe Island (marked in Fig. 1) of 59 cm, and so were aware of the general amplitude of the M_2 tide in the Tasman Sea. It is possible that the Tasman Sea is a sensitive area in the numerical modelling

Fig.5

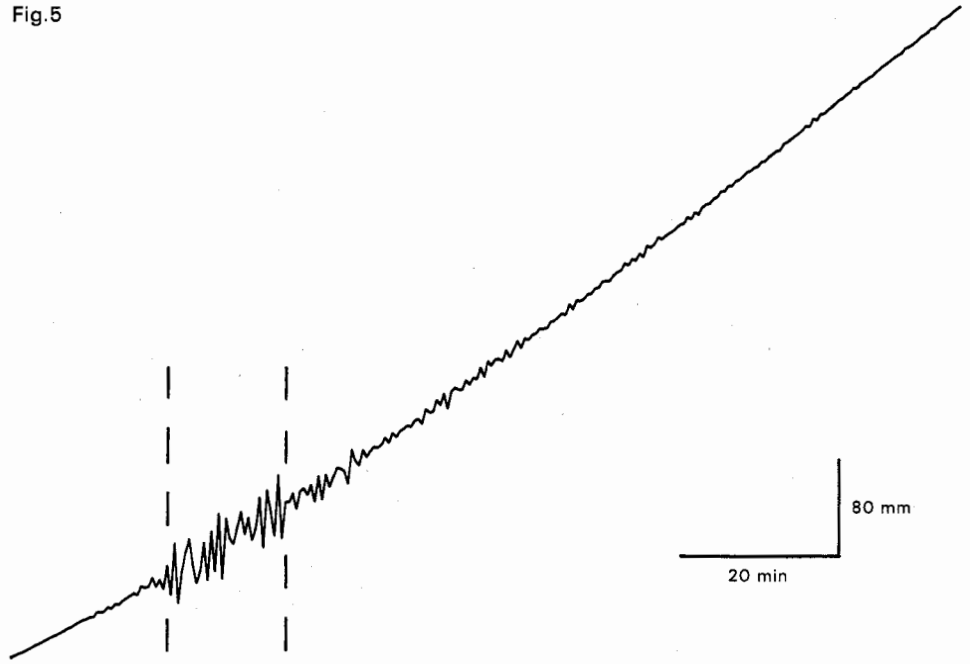

Fig. 6

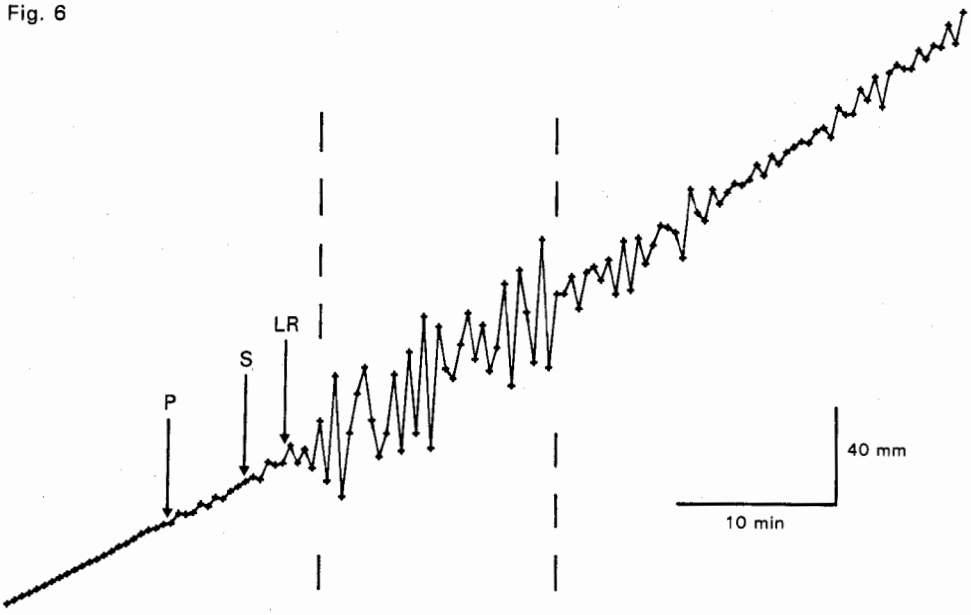

Figs 5 and 6. Plot of the pressure record, joining successive data points, for a 2-h period (*Fig. 5*) and for a 1-h period (*Fig. 6*) starting at 21 h 28 min 50 s on 7 February 1984 UT. Between the two vertical lines, the pressure-fluctuation data are incomplete and may be of greater amplitude than the points plotted. In Fig. 6, the arrows mark the expected arrival times of major seismic phases from the Solomon Islands earthquake, which occurred at 21 h 33 min 20·5 s UT. In this figure, each pressure datum is marked by a small cross; data points are $28\frac{1}{8}$ s apart in time, and their timing is known to an accuracy of 1 s.

of global tides, so that observations from it become valuable to test the accuracy of global models. It is, of course, necessary for such global models to be based on grid sizes fine enough to faithfully represent the Tasman Sea.

The Event of 7 February 1984

Detailed inspection of the data makes very apparent an unusual pressure event occurring on 7 February 1984. This event is shown enlarged in Fig. 5. The signal is reminiscent of the earthquake signals previously detected by seafloor pressure recorders of the same design (Filloux 1980, 1982, 1983) and a review of catalogues of earthquake activity for the duration of recording (Anon. 1984) reveals a major earthquake of magnitude Mb = 7·5 to have occurred in the Solomon Islands on 7 February 1984. The earthquake occurred at time 21 h 33 min 20·5 s UT, at depth 14 km, and at epicentre coordinates 9·924°S.,160·455°E. The site of this epicentre is also marked on Fig. 1.

The angular distance between origin and recording site is 28·5°, so that on the basis of the Jeffreys–Bullen travel times (as presented in Simon 1968) the main seismic phases would be expected to arrive at the following times, predicted to the nearest second:

primary, P: 21 h 39 min 15 s
secondary, S: 21 h 43 min 59 s
surface Rayleigh, LR: 21 h 46 min 52 s.

Fig. 6 shows a further enlargement of Fig. 5. The expected times of arrival of the earliest seismic phases are marked, to aid interpretation. Evidently, the P-phase has been recorded, and also possibly the S-phase. The later strong signal is most likely caused by arrival of Rayleigh 'surface' seismic waves, initially expected at the time indicated by the arrow LR. With data points at $28\frac{1}{8}$-s intervals, each recording a mean value for the preceding $28\frac{1}{8}$-s period, the individual wave forms are not traced through by the data. Further, due to the unusual nature of this pressure event in relation to the instrument design and intention, and the data compacting scheme used for the present observations, the recorded data are incomplete in the period marked as such in Figs 5 and 6. In this interval the pressure changes between successive data points are too great to be recovered from the recorded observations (though they would have been fully sensed by the instrument at the time). With the recording system as used for the present experiment, then, there is thus no way of recovering the maximum amplitude of this pressure event at the seafloor site.

The obvious strength of the signal interpreted as caused by Rayleigh waves suggests, however, that the excitation of the seafloor by the seismic waves could cause resonance in the ocean, with signal reflected between seafloor (exciting antinode) and sea-surface (node due to acoustic mismatch across the sea–air interface). For the known depth of seawater, 4780 m, an oceanic sound speed of 1500 m s^{-1} predicts a resonant period of 12·7 s, which is certainly in the surface-wave energy band of typical seismic signals from strong near-surface earthquakes (such as the Solomon Islands event of 7.ii.1984). While the pressure instrument is not designed for seismic detection, it does have a very flat frequency response up to about 1 Hz, compatible with recording seismic events. Furthermore, as the pressure instrument records ambient water pressure, its mechanical response is independent of the firmness of its coupling with the ocean floor.

The earthquake signals arrived at the pressure instrument at an otherwise very quiet time. This circumstance allows the P and S signals arriving before the surface-wave signals to be detected, and also allows the observation of later arrivals for at least 2 h after the main disturbance. Some such later arrivals may be discerned in Fig. 5. A recent discussion of the noise limits to seismic detection by pressure fluctuations on the deep seafloor is given by Webb and Cox (1984).

Had the earthquake excited tsunami, these would have been expected at the pressure instrument approximately 4 h after the seismic signal. Inspection of the data for this time has not revealed an obvious tsunami signal; however, the presence of a weak signal is not precluded by this inspection.

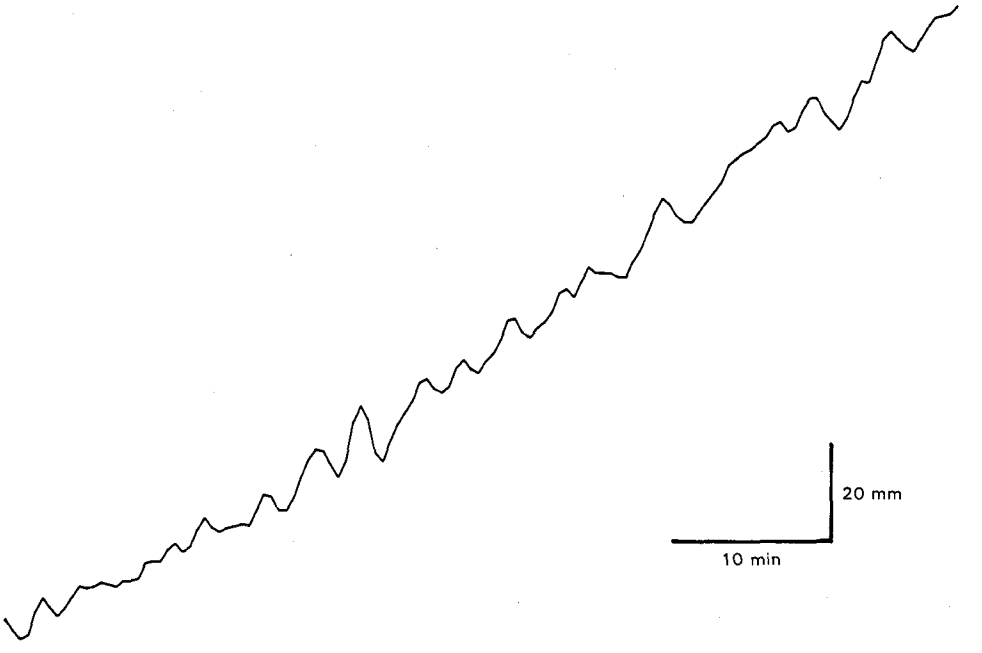

Fig. 7. Plot of the pressure record, joining successive data points, for a 1-h period starting at 12 h 53 min 12 s on 25 February 1984 UT. The signal shown is an example of relatively strong high-frequency pressure fluctuations on the seafloor.

Short-period Signals

As observed by Filloux (1980, 1983) when recording in the Pacific Ocean, the pressure instruments record also short-period low-amplitude signals of variable strength. At times these signals are quiet; a good example is the background signal before arrival of the seismic signal in Fig. 6. At other times the signals are relatively strong; as shown, for example, in Fig. 7.

The example in Fig. 7 has a peak-to-peak range of order 10 mm in equivalent hydrostatic head, and a period with the time scale of several minutes. More work remains to be done on the analysis of such signals, but the most likely explanation, following Filloux (1980, 1983), is that they are due to the effects of surface gravity waves of very long wavelength. Such waves are wind generated, of long period, and their pressure effects suffer little attenuation down to the seafloor. Further clarification of the origin of the signals may be possible by examining them for correlation with the weather patterns recorded for the Tasman Sea, during the time of the seafloor pressure observations.

Discussion

The open-ocean tidal data presented in this paper are the first such observations known for the Tasman Sea. The observed amplitudes and phases are generally consistent with the predictions of the Schwiderski (1980) models, but the differences observed may be useful in refining the latter. There is a wide range in the amplitude of the M_2 component amongst tidal models for

the region, which appears to be a sensitive area in the construction of global tide models. Thus the present results should also be of value in refining both local models, such as those of Bye and Heath (1975), and theoretical global models, such as those of Accad and Pekeris (1978). The recorded data also contain information on tidal components beyond that presented in Tables 1 and 2, and work on the determination of this further information is currently in progress.

Finally, as for the previous data recorded by such instruments in the Pacific Ocean, there are a number of other valuable aspects of the observations, not yet fully explored in the present paper. In particular, one of these aspects is the pressure fluctuations on the seafloor thought to be due to wind-generated long-period surface waves. Since the latter can travel over world-wide distances, the recorded signals may contain useful information on oceanic and meteorological processes.

Acknowledgments

We thank first the Hydrographer, Royal Australian Navy, for making the deployment of the pressure recorder possible by providing ship time. We thank particularly the personnel of HMAS *Cook* for their skilful launching and recovery of the instrument, and for their hospitality to us while on board ship. H. Moeller, G. Pezzoli and T. Koch of the Scripps Institution of Oceanography were essential members of the experimental team. The project was run under the U.S./Australian Agreement for Science and Technology, and U.S. participation was supported by National Science Foundation grants OCE 83-01216 and OCE 83-12339.

At the Australian National University, the encouragement and interest in the project of A. L. Hales, K. Lambeck, M. W. McElhinny, A. E. Ringwood and J. S. Turner have been much appreciated. More widely, we have benefited from discussions on the project with V. T. Buchwald, J. A. T. Bye, R. Coleman, R. W. Griffiths, G. N. Ivey, I. S. F. Jones, G. W. Lennon and J. H. Middleton.

N.L.B. and I.J.F. are the recipients, respectively, of an Australian Commonwealth Postgraduate Research Award and an Australian National University Postgraduate Scholarship.

References

Accad, Y., and Pekeris, C. P. (1978). Solution of the tidal equations for the M_2 and S_2 tides in the world oceans from a knowledge of the tidal potential alone. *Philos. Trans. R. Soc. Lond. Ser. A* **290**, 235–66.

Anon. (1984). Preliminary determination of earthquake epicentres, list no. 6-84 of 1 March 1984. Issued by the United States Department of the Interior, Geological Survey.

Bye, J. A. T., and Heath, R. A. (1975). The New Zealand semi-diurnal tide. *J. Mar. Res.* **33**, 423–42.

Doodson, A. T., and Warburg, M. D. (1941). 'Admiralty Manual of Tides.' (The British Hydrographic Department: London.)

Filloux, J. H. (1980). Pressure fluctuations on the open ocean floor over a broad frequency range: new program and early results. *J. Phys. Oceanogr.* **10**, 1959–71.

Filloux, J. H. (1982). Tsunami recorded on the open ocean floor. *Geophys. Res. Lett.* **9**, 25–8.

Filloux, J. H. (1983). Pressure fluctuations on the open ocean floor off the Gulf of California: tides, earthquakes, tsunamis. *J. Phys. Oceanogr.* **13**, 783–96.

Filloux, J. H. (1984). Semidiurnal amphidrome of the northeast Pacific: where? *Mar. Geophys. Res.* **7**, 247–66.

Godin, G. (1972). 'The Analysis of Tides.' (University of Toronto Press: Toronto.)

Graham, H. (Ed.) (1984). New evidence sought on continental drift. *Aust. Phys.* **21**, 79–80.

Parke, M. E., and Hendershott, M. C. (1980). M_2, S_2, K_1 models of the global ocean tide on an elastic earth. *Mar. Geodesy* **3**, 379–408.

Schwiderski, E. W. (1979). Global ocean tides, Part II: the semi-diurnal principal lunar tide (M_2). Atlas of tidal charts and maps. Report NSWC TR 79-414. Naval Surface Weapons Center, Dahlgren, Virginia.

Schwiderski, E. W. (1980). On charting global ocean tides. *Rev. Geophys. Space Phys.* **18**, 243–68.

Schwiderski, E. W. (1981*a*). Global ocean tides, Part V: the diurnal principal lunar tide (O_1). Atlas of tidal charts and maps. Report NSWC TR 81-144. Naval Surface Weapons Center, Dahlgren, Virginia.

Schwiderski, E. W. (1981*b*). Global ocean tides, Part VI: the semi-diurnal elliptical lunar tide (N_2). Atlas of tidal charts and maps. Report NSWC TR 81-218. Naval Surface Weapons Center, Dahlgren, Virginia.

Schwiderski, E. W. (1981*c*). Global ocean tides, Part IX: the diurnal elliptical lunar tide (Q_1). Atlas of tidal charts and maps. Report NSWC TR 81-224. Naval Surface Weapons Center, Dahlgren, Virginia.

Simon, R. B. (1968). 'Earthquake Interpretations.' (Colorado School of Mines: Golden, Colorado.)

Webb, S., and Cox, C. S. (1984). Pressure and electric fluctuations on the deep seafloor: background noise for seismic detection. *Geophys. Res. Lett.* **11**, 967–70.

Zahel, W. (1977). The influence of solid earth deformations on semi-diurnal and diurnal oceanic tides. In 'Tidal Friction and Earth's Rotation'. (Eds P. Brosche and J. S. Sünderman.) p. 98. (Springer: New York.)

Manuscript received 27 March 1985, accepted 9 August 1985